

Structural relaxation in Si and Ge nanocrystallites: Influence on the electronic and optical properties

H.-Ch. Weissker, J. Furthmüller, and F. Bechstedt

Institut für Festkörperteorie und Theoretische Optik, Friedrich-Schiller-Universität, Max-Wien-Platz 1, D-07743 Jena, Germany

(Received 12 November 2002; published 10 June 2003)

A complex atomic relaxation pattern for hydrogen-saturated Ge and Si nanocrystallites with diameters between 10 and 25 Å has been found by means of *ab initio* calculations. While the bonds at the center of the nanocrystals expand beyond their length in the corresponding bulk material, the bonds near the surface are shortened. The average bond lengths decrease. The atoms at the surface facets move inward, those at the edges and corners outward, leaving the volume of the crystallite almost unchanged. As a consequence of the structural relaxation, the pair excitation energies increase as compared to the values for the respective ideal structures, and they do so stronger for Ge than for Si. The main effect on the overall absorption spectra is an upward shift of the different spectral features. Most important for Ge crystallites is the change of the energetic ordering of the electronic states close to the HOMO-LUMO (highest occupied molecular orbital–lowest unoccupied molecular orbital) gap, leading their radiative lifetimes to decrease by orders of magnitude.

DOI: 10.1103/PhysRevB.67.245304

PACS number(s): 73.22.-f, 61.46.+w, 78.67.-n

I. INTRODUCTION

Si and Ge nanostructures are in the focus of both fundamental and applied research because of their potential for Si-based optoelectronics. Effects due to spatial quantization promise to overcome the limitations of the indirect-gap semiconductors for photoelectronic applications. In fact, even optical gain has been achieved in Si nanocrystals.¹

Nanostructured Ge and Si systems can be fabricated by many different methods, leading to a number of substantially different systems. Very small, nearly spherical Ge nanocrystals (NC's) have been created, e.g., by rf cosputtering of Ge and SiO₂ with diameters down to 0.9 nm,² as colloidal NC's,³ or by ion implantation in SiC and subsequent annealing.⁴ The nanocrystalline material retains its tetrahedral coordination down to very small sizes,³ albeit possibly with modifications like stacking faults and faceting of the surfaces or interfaces.⁴ Thus, in view of the experimental situation, spherical NC's are very interesting systems.

The NC's in question belong to the intermediate size range. While they are larger than quasimolecular clusters, they are not yet as large as to be treatable as small portions of bulk material with a separate consideration of their surfaces. It is reasonable to assume a bulklike tetrahedral structure inside the crystallites at least starting from some minimum size, since in the limit of large diameters the bulk situation must be reproduced.⁵ However, the actual shape of a NC and the exact atomic positions remain open questions. The shape will be determined by thermodynamic as well as by kinetic effects, depending on the preparation conditions.⁶ While the concept of the Wulff construction⁷ derives the equilibrium shape of crystallites from surface energies, it is only applicable in the limit of macroscopic, or at least mesoscopic, volume. Kinetic aspects cannot be treated using a ground-state theory. However, a ground-state theory for the total energy allows *ab initio* structure optimization. Unfortunately, such structural optimization can be carried out only for tiny NC's consisting of a small number of atoms (cf.,

e.g., Refs. 8–11). Consequently, the theoretical investigation of NC's usually starts from model structures. Taking these as little fragments of bulk material, the question arises as to how these structures relax as compared to the initial ideal geometries. Moreover, in view of possible applications it is of utmost importance to know how the relaxation influences the electronic and optical properties.

Several entirely different methods exist to investigate the relaxation behavior of NC's and quantum dots.¹² The analytical¹³ and the numerical¹⁴ continuum approaches make use of the assumption that the quantum dots are reasonably well represented by macroscopic concepts like stress and strain fields. Obviously, the small structures containing a few hundred atoms will not be amenable to such approaches. An atomistic theory has to be used instead (see Ref. 12 and references therein).

The majority of the theoretical treatments are based on quasispherical NC's. These structures are taken as inputs for the calculation of electronic and optical properties without taking relaxation into account,^{16,15} using empirical and semi-empirical methods to relax the structures before the electronic-structure calculations,¹⁷ or relaxing only the atoms near the NC surface by *ab initio* relaxation.¹¹

In view of the system size, an *ab initio* method is needed to account for the possible structural relaxation effects in the NC's. In the present paper we apply *ab initio* relaxation for all crystallite atoms. We calculate the fully relaxed structures of NC's of up to 363 atoms which corresponds to a diameter of 25 Å. We investigate the relaxation pattern in detail, considering, in particular, the surface facets and edges. In order to quantify the influence of the relaxation effects we compare the electronic and optical properties to those obtained for the ideal structures.

II. MODEL AND METHODS

The calculations are performed within density-functional theory (DFT) in local-density approximation (LDA). We employ the VASP program package¹⁸ and non-norm-conserving

pseudopotentials.¹⁹ A supercell approach is taken in order to use the plane-wave expansion of the eigenfunctions. The electron-electron interaction is described within the parametrization of Perdew and Zunger.²⁰ Nonlinear core corrections are taken into account.²¹ The method yields cubic bulk lattice constants of $a_0 = 5.647 \text{ \AA}$ for Ge and 5.404 \AA for Si. The optical properties are calculated within the independent-particle approximation. The projector-augmented wave (PAW) method²² is used to calculate the transition matrix elements. This approach gives reliable spectra for bulk crystals²³ as well as for NC's.¹⁶

We construct NC's by starting from one atom and adding its nearest neighbors, thereby assuming the tetrahedral coordination of the respective cubic bulk material. Successively adding the nearest neighbors of the surface atoms shell by shell we obtain NC's of $N = 5, 17, 41, 83, 147, 239$, and 363 atoms. The remaining dangling bonds are saturated by H atoms. Thereby N denotes the number of atoms in the NC, disregarding the hydrogen atoms. This or similar construction procedures have been applied by different groups.^{11,15,16} The point group of the resulting NC's is T_d , i.e., inversion is the only missing point-symmetry operation compared to the initial bulk material. This is advantageous with respect to the numerical effort. We use a $2 \times 2 \times 2$ Monkhorst-Pack \mathbf{k} -point mesh which results in one \mathbf{k} point in the irreducible part of the Brillouin zone. Inspection of the NC's reveals that they are not precisely spherical but exhibit small facets at the surface. Basically, their shape is a cube with cut-off corners in such a way that triangular faces arise which connect the midpoints of the rectangles that touch at the respective corner. They have six rectangular faces corresponding to a $\langle 001 \rangle$ orientation as well as eight faces corresponding to a $\langle 111 \rangle$ orientation. However, the construction procedure results in two different situations, alternating with an increasing number of shells. Either the six $\{001\}$ faces are quadratic, in which case the $\{111\}$ facets are of the same size. This is the case for the NC's of $N = 17, 83, 239$, etc. atoms. Alternatively, for the NC's of $N = 41, 148, 363$, etc. atoms, the six $\{001\}$ faces are rectangular with edge lengths differing by one atom. In these cases, two different kinds of triangular $\{111\}$ facets arise. Even in the first case of equal edge lengths of the $\{111\}$ facets, they are inequivalent due to the construction procedure.

We use the supercell method with simple-cubic cells, the size of which corresponds to 216, 512, or 1000 atoms of bulk material, depending on the size of the NC in question. Thus for Ge we use edge lengths of 16.9, 22.6, and 28.2 \AA . Keeping the T_d symmetry, ionic relaxation is carried out for all atoms in the NC's. It is expected to yield valid results for changes of bond lengths and bond angles, since this procedure does reasonably describe the bulk elastic properties despite the neglect of temperature effects.

In order to describe electronic pair excitations we use an occupation constraint. To model the electron-hole pair with the lowest excitation energy, we place a hole in the HOMO (highest occupied molecular orbital) and an electron in the LUMO (lowest unoccupied molecular orbital) state of the crystallite. In the spirit of a Δ -self-consistent-field method (Δ SCF),^{24,25} the difference between the total energy of the

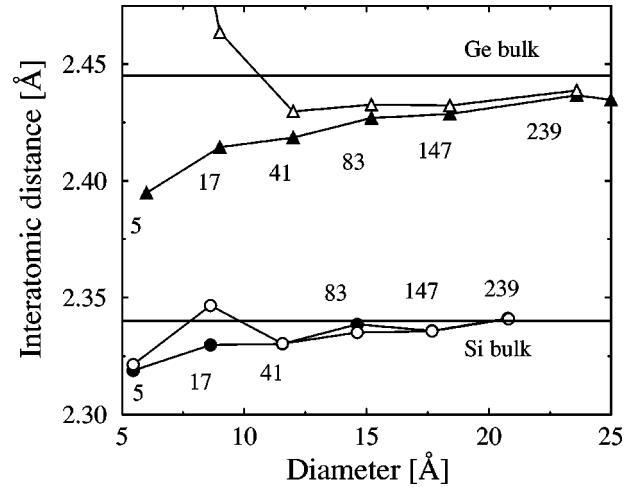


FIG. 1. Interatomic distances in the Ge (triangles) and in the Si (circles) NC's. Filled symbols: ground-state results, empty symbols: results of the relaxation with one electron-hole pair present. The numbers of Ge (Si) atoms in the crystallites are indicated. The horizontal lines indicate the calculated bulk interatomic distances.

excited system and the total energy of the ground state is the excitation energy of the electron-hole pair, which accounts for the Coulombic electron-hole interaction as well as for self-energy effects.

The same occupation constraint is used in order to account for the structural effects of a pair excitation. For the excited electronic configuration, the ionic relaxation is carried out once more. The resulting geometry represents that of the excited NC. The pair excitation energies of the excited-state geometry are calculated by means of the Δ SCF method for the excited structure without ionic relaxation. The difference between the two excitation energies yields the structural contribution to the luminescence Stokes shift which will be presented elsewhere.²⁶

III. STRUCTURE OF RELAXED NANOCRYSTALLITES

A. Bond lengths

The geometry does not change significantly. The bonds are only shortened or stretched, respectively. The average bond lengths of the relaxed NC's are shown in Fig. 1 as a function of the NC diameter. Throughout the paper, we study the Ge-Ge and Si-Si bonds but disregard the Ge-H and Si-H bonds of the hydrogen saturation. The diameter indicated in Fig. 1 is that of a perfect sphere with the same volume as the model structure, where each atom has been assigned its bulk volume $a_0^3/8$. For the ground-state geometry, the average bond lengths are consistently shorter than the respective bulk values. Similar contraction effects have been observed in porous silicon.²⁷ A very recent theoretical molecular-dynamics study⁵ agrees roughly with our findings with respect to the averages. However, under oxygen exposure this contraction turns into an expansion.²⁷ The effect is obviously dependent on the surface saturation. Annealing of porous silicon also leads to nanostructured Si with shortened bonds.²⁸ It has

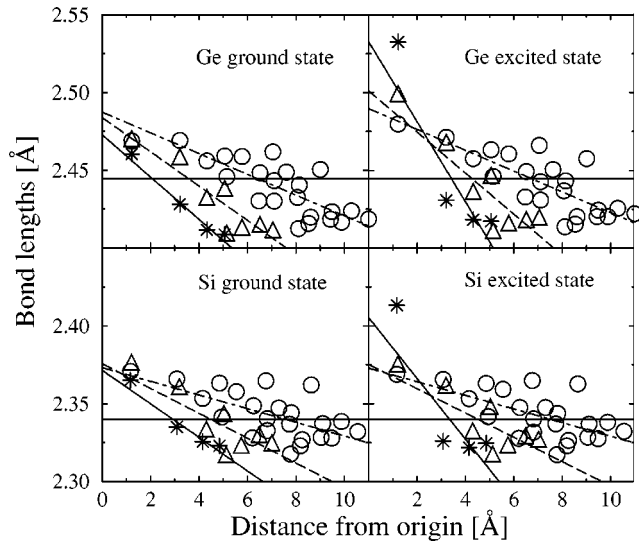


FIG. 2. Individual bond lengths in the NC's plotted against the distance from the center. Asterisks: 41-atom NC's; triangles: 83-atom NC's; circles: 239-atom NC's. The linear fits are given as solid (41), dashed (83), and dot-dashed (239) lines. The horizontal lines are the calculated bulk interatomic distances.

been explained as a consequence of the surface stress.²⁷ The effect is much stronger in the Ge than in the Si NC's. While the average Si interatomic distances have already reached their bulk limit for NC's with diameters of about 20 Å, the bond-length reduction is still substantial (0.35%) for Ge NC's of the same size.

For the excited-state geometry calculated with an electron-hole pair in the crystallite, the situation is more complex. The picture suggests that there might be two mutually counteracting effects on the bond lengths in Fig. 1. The first one is the general bond-length reduction as for the ground state. The second, however, is a tendency of increasing bond lengths with electronic excitation, increasing with decreasing NC size. For the Ge NC's, this leads to a consistent picture. For Si, however, the results with respect to the excitation effect are not so uniform. This might be partly due to the stronger bonds in Si as compared to Ge. Moreover, the symmetry of the LUMO state in the Si NC's is different from that of the Ge NC's, reflecting the strong contributions from the X points of the bulk Si band structure. Thus the symmetry of the lowest pair excitation and hence its effect on the structural relaxation is different in Ge and Si NC's. Special care has to be taken in the discussion of the results for the smallest NC's of 5 and 17 atoms. These represent moleculelike structures rather than NC's and might be governed by completely different mechanisms⁵ which can change their symmetry entirely.²⁹

In order to obtain a more detailed understanding of the geometrical relaxation in the NC's, in Fig. 2 we plot the individual bond lengths against their distance from the center of the NC. In this way we obtain a bond-length distribution similar to the strain-field representation of continuum theory. The bond-length distribution of the NC's is much more complex than can be represented by the average values of Fig. 1. In general, the bond lengths are longest near the center of the

NC, while they decrease further away from the center. Surprisingly, the bonds at the center are longer than the respective bulk interatomic distances, i.e., there is an expansion of the material inside the NC. Near the surface of the NC's, the bonds are shorter than the respective bulk lengths. While the latter compression might be caused by surface-tension-like effects, the expansion at the center cannot. For oxidized Si particles, Hofmeister *et al.*³⁰ find an expansion for small sizes, while for larger particles they report a contraction. It is thus conceivable that the overall situation is a combination of the surface-stress-like effect which induces contraction, while there is another effect which causes the expansion at the center and, when the surface stress is reduced, e.g., by oxidation, the expansion of the whole NC. This is corroborated by the fact that many groups have found strong influences of the surface saturation on the NC properties.^{27,31–33}

The straight lines in Fig. 2 are linear fits of the respective data. However, two remarks are in order. First, due to the symmetry of the NC's, each of the data points in Fig. 2 represents many bonds of the same length. No attempt has been made to show this multiplicity in the figure. Second, even though we use a linear fit, we do not claim that the dependence is in fact linear. We merely demonstrate the general trend. The slope of the lines decreases with increasing NC size. However, the results show that the bulk limit (zero slope at the bulk bond lengths) has not even nearly been reached for even the largest Si crystallites. That means that the apparent convergence towards the bulk interatomic distance of the larger Si NC's of Fig. 1 is an effect of the averaging procedure rather than real convergence.

To investigate the difference in the relaxation behavior of Si and Ge NC's one can compare the relative bond lengths d/d_{bulk} . For the two largest crystallites we find that while the expansion in the center is slightly stronger for Si than for Ge, the bond-length reduction towards the surfaces is more pronounced for Ge. This explains the behavior of the average bond lengths in Fig. 1.

For the excited-state relaxed systems, the situation is not very different. The slope of the decrease of the bond lengths with increasing radial distance becomes steeper. However, the general effects found for the ground-state geometries are not changed. We note that the discussion of only the average bond lengths can be misleading. For instance, the 41-atom Si NC which does not show any change in the average bond length with the excitation exhibits changes in the individual bond lengths comparable to the changes in the other NC's.

B. Surface shape

The rectangular facets of the largest NC of the present work consist of 20 atoms. In general, the atoms along the edges and at the corners move outward (though not necessarily radially) with respect to the ideal positions, whereas the atoms on the surface facets move inward or, for the larger NC's, move hardly at all. The relaxation thus increases the deviations from the spherical shape which indicates that surface stress alone cannot be responsible for the surface relaxation. The displacements are shown in Fig. 3(a) where a schematic view of the 239-atom Ge NC is presented.

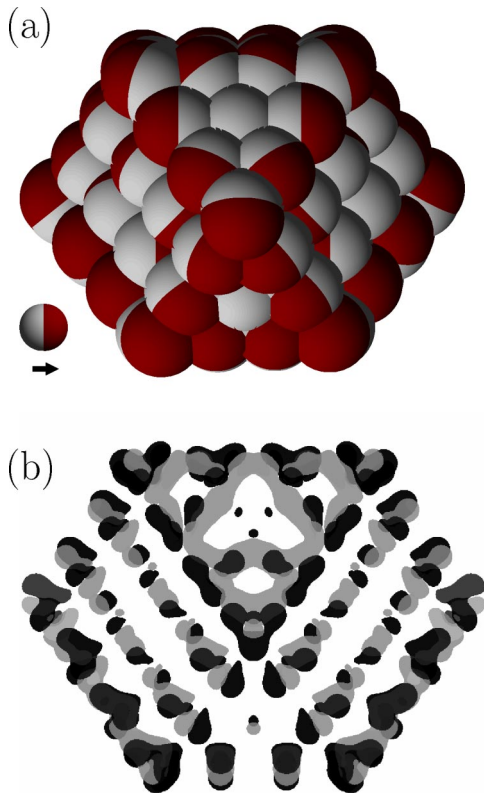


FIG. 3. (a) Schematic view of the NC of 239 Ge atoms. The direction of the displacement during the relaxation is indicated as shown in the legend. (b) Difference of the electron densities before and after the relaxation. Electron transfer takes place from the grey (negative difference) to the black (positive difference) regions.

The atomic relaxation is accompanied by a change of the electrostatic energy. In Fig. 3(b) the difference between the total electron densities for the ideal and the relaxed NC's is plotted. Electron transfer takes place from the gray to the black areas. It can be seen that the largest changes take place at the surface, and, especially, along the edges of the facets.

The conclusion that electrostatic forces play some role for the surface relaxation, in particular the inward relaxation on the facets, is supported by analogies to free surfaces. Inward-relaxation effects have been found for both Ge and Si (111):H-2 \times 1 surfaces^{35,34} and for many low-index surfaces

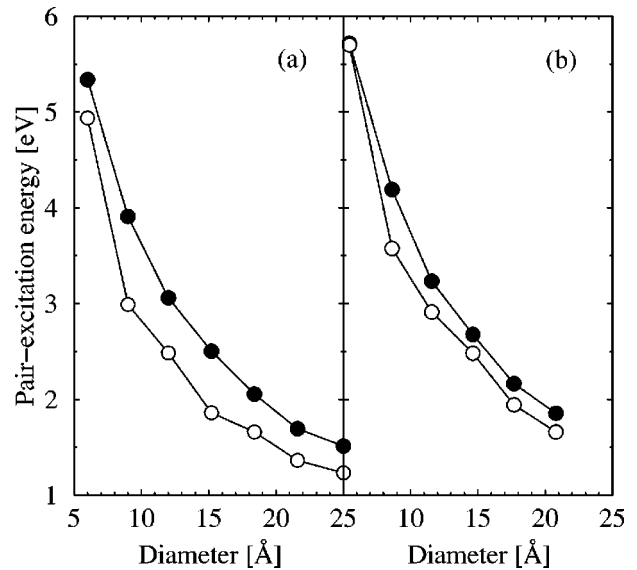


FIG. 4. Pair excitation energies of Ge (a) and Si (b) NC's for the ideal (empty symbols) and the relaxed (filled circles) geometries.

of metals, e.g., the W(100) surface.³⁶ By analogy to H-saturated surfaces³⁵ it is conceivable that a charge transfer towards the H atoms in the Ge-H and Si-H bonds causes a repulsion between the now positively charged Ge or Si atoms, thus contributing to the outward relaxation of the edge and corner atoms.

IV. INFLUENCE OF STRUCTURAL RELAXATION ON ELECTRONIC AND OPTICAL PROPERTIES

A. Lowest pair excitation energies

The effect of the structural relaxation on the lowest pair excitation energies is shown in Fig. 4. The pair excitation energies shift to higher energies when the ionic relaxation is taken into consideration. They do so stronger for Ge than for Si. This is probably connected to the lesser overall reduction of the average bond lengths in Si (cf. Fig. 1). As the wave functions spread over the entire crystallite (see below) it is very likely that they experience such an average effect. It has been shown elsewhere³⁷ that the band gap of Ge NC's increases with increasing hydrostatic pressure, i.e., with short-

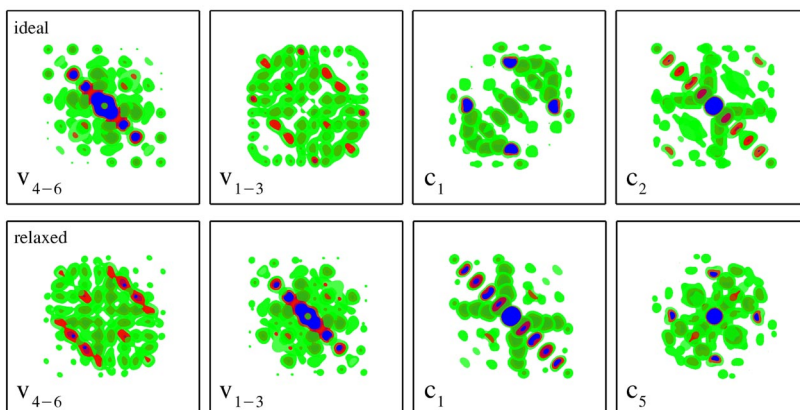


FIG. 5. Plots of the electronic states close to the HOMO-LUMO gap for the ideal (upper panels) and the relaxed (lower panels) Ge crystallite of 83 atoms ($d=15.2$ Å). The notation v_{1-3} means that the highest three valence states are degenerate and therefore represented by their average. Partly transparent isosurfaces of the probability density are shown. The resulting shape has been sectioned along the midplane through the NC and is viewed from the z direction. Thus, besides the contour plot of the values in the mid-plane, the parts of the distribution below that plane are also shown. A triply degenerate state c_{2-4}^{rel} for the relaxed crystallite has not been shown.

TABLE I. Degeneracies of the lowest unoccupied and the highest occupied states for the ideal and the relaxed Ge NC geometries. The notation 3,3 — 1,3,1 means that the two highest occupied states are threefold degenerate, whereas the first empty state is nondegenerate, etc.

Number of Ge atoms	Unrelaxed	Relaxed
5	3,3 — 1,3,1	3,3 — 1,1,3
17	3,3 — 1,3,1	3,3 — 1,3,1
41	3,3 — 1,1,3	3,3 — 1,3,1
83	3,3 — 1,1,3	3,3 — 1,3,1
147	3,3 — 1,3,1	3,3 — 1,3,1
239	3,3 — 1,1,3	3,3 — 1,3,1
363	3,3 — 1,1,3	3,3 — 1,3,1

ened bonds, which is consistent with the above interpretation. However, test calculations showed that this is not the case for Si where an increase of hydrostatic pressure causes an increase in the gap energy, cf. Ref. 37. Thus the increase in the pair excitation energies for the Si NC's cannot be explained simply by the average reduction of the bond lengths.

The atomic relaxation influences the energetic ordering of the single-electron states. Since the photoluminescence (PL) properties are determined by the lowest few optical transitions, it is particularly interesting to investigate the electronic states in the energy region of the HOMO and the LUMO states. We consider the corresponding one-particle wave functions of the 83-atom Ge NC. Their respective probability densities are plotted in Fig. 5(a) for the ideal geometry and in Fig. 5(b) for the relaxed NC. We have shown elsewhere¹⁶ that the HOMO-LUMO transitions of the unrelaxed Ge NC's are forbidden. However, just above the HOMO-LUMO gap, there are very strong optical transitions. In the 83-atom Ge NC they correspond to a transition between the states v_{4-6}^{ideal} and c_1^{ideal} with oscillator strength 0.22 and between the states v_{4-6}^{ideal} and c_2^{ideal} with a value of 0.38. The notation means that the state v_{4-6}^{ideal} is triply degenerate (without spin) and comprises the fourth-, fifth-, and sixth-highest valence states. Accordingly, c_1^{ideal} is the (nondegenerate) lowest unoccupied state. In addition, each state is doubly degenerate because of the spin.

For the relaxed NC, the energetic ordering is changed. While the electronic states are not, strictly speaking, the same as for the unrelaxed system, at least some of them change only very little. Comparison shows that the triply degenerate second-highest state v_{4-6}^{ideal} of the unrelaxed system becomes the HOMO state v_{1-3}^{relaxed} of the relaxed system, thereby remaining almost unchanged. Moreover, the former second-lowest unoccupied state c_2^{ideal} becomes, with slight modifications, the LUMO state c_1^{relaxed} . We mention that there is a state c_{2-4}^{relaxed} (not shown) which is not among those shown for the ideal system.

Thus we have shown that a proper account of the structural relaxation is indispensable in order to calculate the optical properties near the HOMO-LUMO gap correctly. While this has been illustrated for the 83-atom Ge crystallite, the

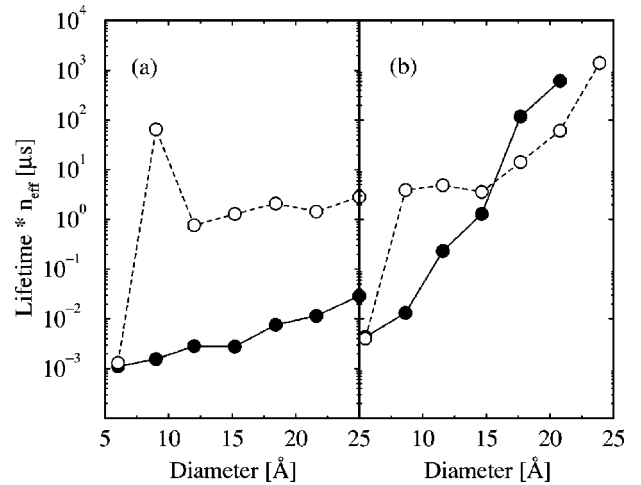


FIG. 6. Radiative lifetimes of Ge(a) and Si(b) crystallites. The values for the relaxed NC's are shown as filled, those for the ideal geometries as empty circles. The refractive index n_{eff} of the nanocrystalline material remains unspecified. Room temperature is assumed.

situation for the other Ge NC's is very similar. In Table I we indicate how the degeneracies of the electronic states around the gap differ for the relaxed and the ideal structure. In contrast to the ideal geometries, strong HOMO-LUMO transitions have been found for all the relaxed Ge NC's. We mention that test calculations treating a really nonspherical Ge NC of somewhat arbitrary symmetry have reproduced the strong transitions at the HOMO-LUMO gap.

In view of the oscillator strengths (not shown) it can be stated that the qualitative difference between Ge and Si NC's found for the ideal structures¹⁶ is not changed by the structural relaxation. Si NC's retain their long tail of extremely weak optical transitions below the onset of appreciable absorption. Hence it does not make much of a difference which of them is lowest. Consequently, the analysis of their order has not been carried out as for the Ge crystallites.

B. Radiative lifetimes and absorption spectra

The strong HOMO-LUMO transitions in the relaxed Ge NC's reduce the radiative lifetimes drastically compared to those of the ideal structures. This effect is shown in Fig. 6. The lifetimes τ for the ideal and the ground-state relaxed geometries have been calculated using an expression which assumes completely thermalized distributions of the excited electrons and holes.³⁸ Consequently, due to the occupation, the lifetimes (or their inverse, the radiative transition probabilities) are governed by the lowest few transitions. For Ge NC's this manifests an extreme influence of the structural relaxation on the lifetimes, changing them by more than two orders of magnitude. For all the larger NC's, beginning with the 41-atom NC, this result is consistent.

For Si NC's, on the other hand, the result is not as uniform. In contrast to Ge, Si NC's have no single strong transitions of particular importance. Therefore we did not attempt to identify individual transitions before and after the relaxation. However, also here substantial changes are found. Figure 6(b) shows that they are smaller than for the Ge crys-

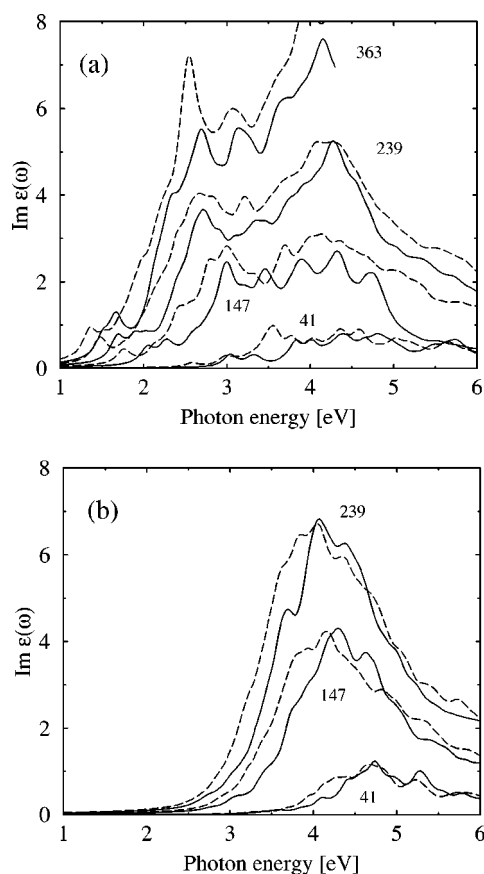


FIG. 7. Imaginary part of the dielectric function of the Ge (a) and Si (b) NC's. The number of atoms in each NC is as indicated. Results for the relaxed NC's are shown as solid, for the ideal geometries as dashed lines. For better visibility, the spectra have been scaled¹⁶ such as to represent the respective filling factor in the supercell corresponding to 1000 bulk atoms.

tallites. Moreover, the lifetimes are not always reduced as for the Ge crystallites. In general, apart from the smallest crystallites of only a few atoms, the radiative lifetimes of the Si NC's are much larger than those of the Ge crystallites. This is in agreement with the trend of measurements of the radiative lifetimes for $\text{Si}_{1-x}\text{Ge}_x$ alloy NC's.^{39,40}

The effects of the structural relaxation on the absorption spectra are demonstrated in Fig. 7. We present the imaginary part of the dielectric function for both Ge and Si NC's. While there is some shift and possibly a redistribution of oscillator strengths between the results for the relaxed and the ideal structure, the overall appearance of the spectra does not change strongly. Comparing the spectra and the excitation

energies of Fig. 4 it can be seen that the onset of the absorption (corresponding to the excitation energies) shifts stronger than some of the high-energy features. This might explain why the absorption spectra for unrelaxed Ge NC's in Ref. 16, in particular the broad high-energy features related to the bulk E_1 and E_2 critical point energies, agree quite well with experiment, even though in the present work we find a substantial influence of the relaxation on the lowest transition energies. There is no substantial difference in the effects of the ionic relaxation on the absorption spectrum of Si and Ge NC's.

V. CONCLUSION

Using an *ab initio* method we have investigated the lattice relaxation and its effects on the electronic and optical properties of H-saturated, nearly spherical nanocrystals with small surface facets. The average bond length decreases as compared to the respective bulk material. The interior of the crystallites undergoes an expansion, the bond lengths near the center are larger than those in the respective bulk material. However, towards the surface the bond lengths decrease below the bulk bond length. The atoms on the facets behave differently from those along their edges. Electronic excitation does not change these findings qualitatively. The relaxation pattern at the surfaces is complex. The edges and the corners of the small surface facets move outward, while the atoms on the facets move inward as compared to the ideal structure.

Depending on the desired quantity and, of course, also on the system, the proper consideration of structural relaxation can be extremely important, as it is for the radiative lifetimes. The energetic order of the electronic states has been found to change in the Ge crystallites, making the very strong transitions above the HOMO-LUMO transition of the ideal structures the lowest ones. This reduces the radiative lifetimes of the Ge NC's drastically as compared to the ideal-structure result. The optical-absorption spectra are mainly shifted to higher energies by the effects of the lattice relaxation.

ACKNOWLEDGMENTS

Interesting discussions with J.-M. Wagner are gratefully acknowledged. We acknowledge financial support from the Deutsche Forschungsgemeinschaft (Project No. Be1346/12-1) and from the European Community in the framework of the Research Training Network NANOPHASE (Contract No. HPRN-CT-2000-00167).

¹L. Pavesi, L. Dal Negro, C. Mazzoleni, G. Franzo, and F. Priolo, *Nature (London)* **408**, 440 (2000).

²S. Takeoka, M. Fujii, S. Hayashi, and K. Yamamoto, *Phys. Rev. B* **58**, 7921 (1998).

³J.P. Wilcoxon, G.A. Samara, and P.N. Provencio, *Phys. Rev. B* **60**, 2704 (1999).

⁴Ch. Schubert, U. Kaiser, A. Hedler, W. Wesch, T. Gorelik, U.

Glatzel, J. Kräusslich, B. Wunderlich, G. Hess, and K. Goetz, *J. Appl. Phys.* **91**, 1520 (2002).

⁵L. Pizzagalli, G. Galli, J.E. Klepeis, and F. Gygi, *Phys. Rev. B* **63**, 165324 (2001).

⁶M. Meixner, E. Schöll, V.A. Shchukin, and D. Bimberg, *Phys. Rev. Lett.* **87**, 236101 (2001).

⁷G. Wulff, *Z. Kristallogr.* **34**, 449 (1901).

- ⁸C. Noguez and S.E. Ulloa, Phys. Rev. B **56**, 9719 (1997).
- ⁹A.A. Shvartsburg, B. Liu, Zhong-Yi Lu, Cai-Zhuang Wang, Martin F. Jarrold, and Kai-Ming Ho, Phys. Rev. Lett. **83**, 2167 (1999).
- ¹⁰J. Wang, G. Wang, and J. Zhao, Phys. Rev. B **64**, 205411 (2001).
- ¹¹I. Vasiliev, S. Ögüt, and J.R. Chelikowsky, Phys. Rev. Lett. **86**, 1813 (2000).
- ¹²Y. Kikuchi, H. Sugii, and K. Shintani, J. Appl. Phys. **89**, 1191 (2001).
- ¹³F. Glas, J. Appl. Phys. **90**, 3232 (2001).
- ¹⁴O.G. Schmidt, K. Eberl, and Y. Rau, Phys. Rev. B **62**, 16 715 (2000).
- ¹⁵F.A. Reboredo, A. Franceschetti, and A. Zunger, Phys. Rev. B **61**, 13 073 (2000).
- ¹⁶H.-Ch. Weissker, J. Furthmüller, and F. Bechstedt, Phys. Rev. B **65**, 155327 (2002); **65**, 155328 (2002).
- ¹⁷A. Zunger, Phys. Status Solidi B **224**, 727 (2001).
- ¹⁸G. Kresse and J. Furthmüller, Comput. Mater. Sci. **6**, 15 (1996); Phys. Rev. B **54**, 11 169 (1996).
- ¹⁹J. Furthmüller, P. Käckell, F. Bechstedt, and G. Kresse, Phys. Rev. B **61**, 4576 (2000).
- ²⁰J.P. Perdew and A. Zunger, Phys. Rev. B **23**, 5048 (1981).
- ²¹S.G. Louie, S. Froyen, and M.L. Cohen, Phys. Rev. B **26**, 1738 (1982).
- ²²P.E. Blöchl, Phys. Rev. B **50**, 17 953 (1994).
- ²³B. Adolph, J. Furthmüller, and F. Bechstedt, Phys. Rev. B **63**, 125108 (2001).
- ²⁴S. Ögüt, J.R. Chelikowsky, and S.G. Louie, Phys. Rev. Lett. **79**, 1770 (1997); R.W. Godby and I.D. White, *ibid.* **80**, 3161 (1998); A. Franceschetti, L.W. Wang, and A. Zunger, *ibid.* **83**, 1269 (1999).
- ²⁵R.O. Jones and O. Gunnarsson, Rev. Mod. Phys. **61**, 689 (1989).
- ²⁶H.-Ch. Weissker, J. Furthmüller, and F. Bechstedt (unpublished).
- ²⁷D. Buttard, G. Dolino, C. Faivre, A. Halimaoui, F. Comin, V. Formoso, and L. Ortega, J. Appl. Phys. **85**, 7105 (1999).
- ²⁸Y.H. Ogata, N. Yoshimi, R. Yasuda, T. Tsuboi, T. Sakka, and A. Otsuki, J. Appl. Phys. **90**, 6487 (2001).
- ²⁹L. Reining, O. Pulci, M. Palummo, and G. Onida, Int. J. Quantum Chem. **77**, 951 (2000).
- ³⁰H. Hofmeister, F. Huiken, and B. Kohn, Eur. Phys. J. D **9**, 137 (1999).
- ³¹M.V. Wolkin, J. Jorne, P.M. Fauchet, G. Allan, and C. Delerue, Phys. Rev. Lett. **82**, 197 (1999).
- ³²F.A. Reboredo and A. Zunger, Phys. Rev. B **63**, 235314 (2001).
- ³³A.B. Filonov, S. Ossicini, F. Bassani, and F. Arnaud d'Avitaya, Phys. Rev. B **65**, 195317 (2002).
- ³⁴E. Kaxiras and J.D. Joannopoulos, Phys. Rev. B **37**, 8842 (1987).
- ³⁵W. Mönch, *Semiconductor Surfaces and Interfaces*, 2nd ed. (Springer, Berlin 1995).
- ³⁶E. Wimmer and A.J. Freeman, in *Electronic Structure*, edited by K. Horn and M. Scheffler, Handbook of Surface Science, Vol. 2 (Elsevier, Amsterdam, 2000), p. 1.
- ³⁷H.-Ch. Weissker, J. Furthmüller, and F. Bechstedt, Mater. Sci. Eng. B (to be published).
- ³⁸C. Delerue, G. Allan, and M. Lannoo, Phys. Rev. B **48**, 11 024 (1993).
- ³⁹S. Takeoka, K. Toshikiyo, M. Fujii, S. Hayashi, and K. Yamamoto, Phys. Rev. B **61**, 15 988 (2000).
- ⁴⁰H.-Ch. Weissker, J. Furthmüller, and F. Bechstedt, Phys. Rev. Lett. **90**, 085501 (2003).